Soft Matter

ARTICLE TYPE

Cite this: DOI: 00.0000/xxxxxxxxxx

Physics-informed constitutive modelling of hydrated biopolymer aerogel networks

İsmail Doğan Külcü[a] and Ameya Rege*[b]

Received Date
Accepted Date

DOI: 00.0000/xxxxxxxxxx

Hydration induces significant structural rearrangements in biopolymer aerogels, resulting in a completely different mechanical behaviour compared to the one in the dry state. A network decomposition concept was earlier introduced to account for these changes, wherein the material network was decomposed into an open-porous aerogel one and a hydrogel-like one. Recent experimental evidences have supported this idea of the formation of a hydrogel-like network. Using these observations as a basis, in this paper, we present a micromechanical model describing the effect of hydration on the structural and mechanical properties of aerogels. The aerogel network is modelled based on the mechanics of their pore-walls, while the hydrogel-like network is modelled based on the statistical mechanics of their polymer chains by means of the Arruda-Boyce eight-chain model. The influence of diverse structural and material parameters on the mechanical behaviour is investigated. The effect of different degrees of wetting, from a pure aerogel to a pure hydrogel, is captured by the model. The results are shown to be in good agreement with available experimental data.

Aerogels from biopolymer sources exhibit highly open-cellular nanoporous morphologies, that exhibit a three-dimensionally interconnected fibrillar network. Amongst all the studied biopolymer aerogels, those from polysaccharide sources are the most well investigated.[1] While a generally increasing trend is observed in the number of publications on aerogels, the trend is found to be exponential for the cases specific to those of biopolymer ones.[2] This rapid development in the field can be attributed to the ever increasing range of possible applications, from thermal insulation, filtering, catalysis, drug delivery, to tissue engineering.[3–6] Amongst these, the biomedical applications seem to be driving the research on improving the mechanical properties of biopolymer aerogels. Their porous morphologies can be tailored according to specific applications, since their pore-sizes range from only a few nanometres to hundreds of nanometres. For biomedical storage applications, their chemical, physical and biological stability play a crucial role, especially with respect to the relative humidity.[6]

To describe this stability of the aerogels under hydrated conditions, diverse experimental and theoretical approaches have recently been reported.[7–9] Antonyuk *et al.*[7] investigated the effect of wetting on the mechanical properties of alginate-starch aerogels. With increasing degree of wetting, they observed a stiffening of the mechanical response of the aerogels, as measured under compressive loading. To present an explanation to this stiffening effect, we proposed a constitutive model.[8] There, we decomposed the material network into an aerogel network and a hydrated one. Biopolymers are intrinsically hydrophilic. This is because biopolymers carry bound water which is retained even after moderate drying. It was proposed, that this bound water may result in local accumulation of water upon wetting, resulting in a partial swelling of the polymer backbone. This led us to assume the existence of a hydrated network. Such an assumption is not uncommon.[10] The aerogel network was modelled based on the mechanics of the pore-walls, as was shown by Rege *et al.*,[11] while the hydrated network was described using the Gent model.[12] While the proposed modelling approach was shown to be effective in capturing the stiffening effect, the experimental validation of the network decomposition theory remained incomplete.

Very recently, our modelling assumptions were supported by experimental characterisations presented by Forgács *et al.*.[9] They characterised the effect of hydration on the structural modifications in Ca-alginate aerogels at different states of hydration by small-angle neutron scattering (SANS), liquid-state nuclear magnetic resonance (NMR) spectroscopy, and magic angle spinning (MAS) NMR spectroscopy. They observed the following effects: (1) The primary fibrils of the original aerogel backbone formed hydrated fibres and fascicles, (2) this resulted in a significant increase in the proportion of pore sizes, (3) this increased the fractal dimension of the network, (4) the stiffness and the compressive strength of the hydrated aerogel significantly increased compared to its dry-state properties, (5) beyond a critical state,

[a] *Department of Materials Science and Engineering, İzmir Katip Çelebi University, 35620 İzmir, Turkey*
[b] *Department of Aerogels and Aerogel Composites, Institute of Materials Research, German Aerospace Center, Linder Höhe, 51147 Cologne, Germany; E-mail: ameya.rege@dlr.de*

the Ca-alginate fibres of the backbone disintegrated into well-hydrated chains, which eventually formed a quasi-homogeneous hydrogel-like network, (6) after this state, the porous structure collapsed and the well-defined solid backbone ceased to exist. These conclusions supported our previously introduced network decomposition concept for numerically describing the effect of hydration on the structural and mechanical properties of the aerogels. In our previous work, the hydrated network was modelled by means of a phenomenological Gent model, due to the lack of the support from experimental evidences at that time.

In this paper, we present a micromechanical description of the hydrated aerogel network as well as the open-porous aerogel one. The proposed model uses the new insights from the recent experimental work[9] to build up on and extend the previous one.[8]

In the following, we refer to a fibril as an aggregation of polymer chains that form the pore-walls of the aerogel network. In the dry state, the material network is formed of an interconnected cellular-appearing fibrillar network. These interconnections are also termed as physical entanglements (see Fig. 1 (a)). While the entire fibrillar network uptakes water upon hydration, at certain focal points, there is a significant rearrangement in the network that is observed. This is a result of conformational changes at a molecular level. These changes induce the rearrangement of the primary fibrils of the original dry aerogel backbone into fibres and fascicles (see Fig. 1 (b)). This begins the onset of the formation of a hydrated network within the aerogel one. This rearrangement results in the subsequent increase in the pore-sizes. Thus, the network is decomposed into an aerogel network and a hydrated one.

Aerogel network model is described based on our previous works.[11,13] The network is assumed to be formed of idealised square-shaped cells that are homogeneously distributed through the network. An illustrative fibril and the cell are shown in Fig. 1 (a). The pore-walls are modelled as Euler-Bernoulli beams that undergo bending and axial stretching. The strain energy in a pore wall is expressed as a sum of the bending (ψ_{bn}) and axial (ψ_{st}) effects as

$$\psi_A = \psi_{bn} + \psi_{st}, \tag{1}$$

where,

$$\psi_{bn} = \int_0^l \frac{1}{2}\kappa(\varphi')dl, \;\; \psi_{st} = \int_0^l \frac{1}{2}\mu(u')dl, \tag{2}$$

where φ' and u' represent the curvature and axial strain along the pore-walls. κ and μ denote the bending and stretching stiffness in the pore-walls. The above-defined equations were solved for nonlinear deformation of the walls using elliptic integrals.[13,14] While these equations describe the strain energy in one cell, the aerogel network is made up of many such cells with varying pore sizes. The pore sizes are typically estimated experimentally using the nitrogen sorption isotherms by means of the Barrett-Joyner-Halenda (BJH) model.[15] The so obtained pore-size distributions are then used to obtain a probability density function (PDF) describing the density of the pore-space through the network. The

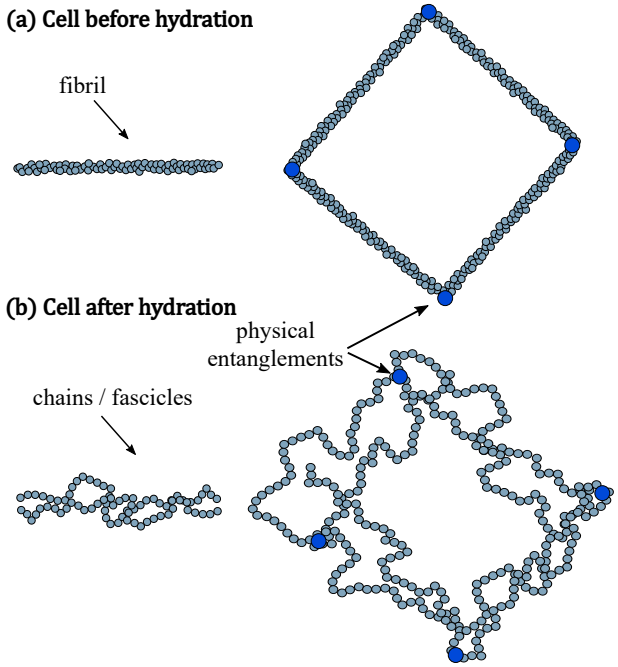

Fig. 1 Illustration of an idealised square-shaped cell (a) before hydration, and (b) after hydration.

experimental PDF is typically non-Gaussian and has been shown to be approximated by means of the generalised beta PDF, which is given as

$$p(l) = \frac{(l-l_{min})^{\alpha-1}(l_{max}-l)^{\beta-1}}{F(\alpha,\beta)(l_{max}-l_{min})^{\alpha+\beta-1}}, \tag{3}$$

where, l_{min} and l_{max} denote the limits of the PDF. Thus, the one-dimensional strain energy in the aerogel network can be expressed as

$$\Psi_A^{\boldsymbol{d}} = \int_{l_{min}}^{l_m} N_0 p(l) \psi_A(\overset{\boldsymbol{d}}{\lambda}, l)dl, \tag{4}$$

where, λ represents the applied micro-stretch to the network and $\boldsymbol{d}$ an arbitrary spatial direction. N_0 denotes the number of micro-cells through the aerogel network in the reference configuration. The parameter l_m specifies the damage evolution through the network. In our model, the pore collapse in the aerogel network is dictated by the critical Euler buckling load in the pore-walls. Once the critical buckling load in a pore-wall is reached, the pore is considered to collapse. Since this critical buckling load $F_{cr} \propto \frac{1}{l^2}$, the pore collapse begins from the larger cells to the smaller ones. This is addressed in more detail in another recent paper.[16]

Hydrated network begins to form upon hydration of the otherwise dry aerogel matrix. This is a result of the water uptake which induces structural rearrangements within the network, where some fibrils disintegrate and re-aggregate to form fascicles resulting in the appearance of a hydrogel-like phase. Therefore, in addition to Ψ_A, the strain energy of the hydrogel-like network must be accounted towards the total strain energy of the hydrated aerogel matrix as well. To reproduce the hyperelastic-like behaviour

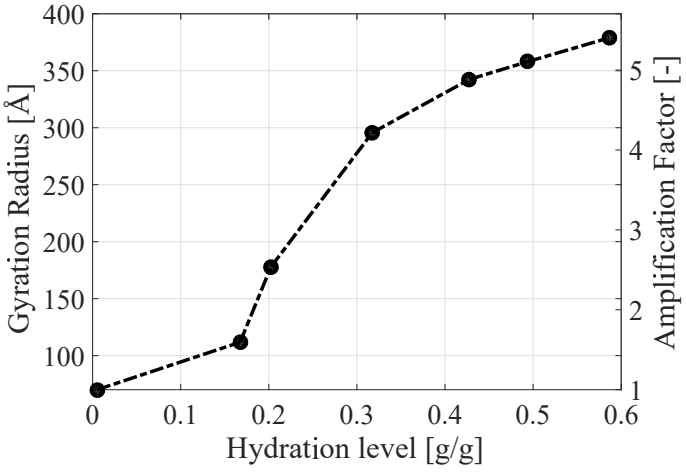

Fig. 2 Relation between the gyration radius[9] and the amplification factor

of the hydrogel-like network,[17,18] the Arruda-Boyce eight chain model (ABecM)[19] was deemed suitable to model its mechanical features.[20] In the ABecM, the entropic energy of a single chain is based on the Langevin statistics, and is expressed as

$$\psi_h = kTn\left(\frac{\bar{r}}{n}\beta + \ln\frac{\Gamma}{\sinh\Gamma}\right), \tag{5}$$

where k is the Boltzmann constant, T is the absolute temperature, n is the chain segment number, $\bar{r}$ is the mean normalised contour length and Γ is the inverse Langevin function. To approximate Γ, the Puso approximation[21] was used.

Moreover, hydration results in the increase of gyration radius and subsequently in the formation of fascicles and fibres from the dry aerogel fibrils.[9] By relating the contour length of an alginate polymer chains with the fibril lengths (see Fig. 1 (b)), the minimum ($\bullet_{min}$) and maximum ($\bullet_{max}$) normalised contour length of alginate chains is written as

$$\bar{r}_{min} = \frac{l_{min}}{\Delta}, \quad \bar{r}_{max} = \frac{l_{max}}{\Delta}, \tag{6}$$

where Δ is the Kuhn length of alginate. By assuming the proportional change in the contour length during the deformation, $\bar{r}$ is represented as

$$\bar{r} = \bar{r}_{min} + \frac{\lambda_h}{\lambda_{max,h}}\left(\bar{r}_{max} - \bar{r}_{min}\right), \tag{7}$$

where λ_h and $\lambda_{max,h}$ are the micro-stretch and the maximal micro-stretch along the deformation, respectively.

As the shortest chain may reach the fully stretched state first in the ABecM, deformation in the hydrogel-like network can be considered to take place from shorter chains to longer ones. This is opposite to what happens in the dry aerogel network. Therefore, the network evolution in the hydrogel-like phase occurs when

$$n_{min} = \bar{r}\nu\lambda_h, \tag{8}$$

where n_{min} and ν are the minimum segment number in the polymer network and the sliding ratio of the polymer right-before the breakage and prevents the singularity that might otherwise appear in the entropic energy of a single chain at the fully-stretched state.[22]

Another remarkable experimental validation of the presented theory concerns the comparison of the size distribution of hydrogel droplets in the alginate aerogel network to that of the generalised beta distribution function used for the cell size distribution.[8,9] They are evidently similar, thus, indicating that hydration appears to follow the same (or at least similar) trend as that of the cell size distribution. Thus, the same probability density function can be used for both networks, eliminating the need to reconstruct an arbitrary chain-size distribution.

Thus, the total energy of the hydrated network is represented by

$$\Psi_H = \xi\Phi N_0 \int_D p(l)\psi_h(\lambda_h, l)dl, \tag{9}$$

where ξ is the amplification multiplier of the number of cells due to the rearrangement of dry-aerogel fibrils into fascicles and fibres, Φ is the normalisation factor calculated based on the network alteration theory[23] and D is the available segment number in the network represented as $D = \{n|\bar{r}\nu < n_{min} < n_{max}\}$.[22] To calculate ξ, the rate of increase of the gyration radius[9] is associated with the amplification factor, as it concerns the structural rearrangements in the dry aerogel matrix upon hydration (see Fig. 2). Thus, more fibrils aggregate to form the hydrogel-like network, thus resulting in larger pores are observed in experiments.

Total network response, Ψ, is then obtained by adding the strain energies of the two networks. To decompose the hydrated aerogel matrix, the hydration level, $\mathscr{H}$ is accounted as

$$\Psi = (1-\mathscr{H})\Psi_A + \mathscr{H}\Psi_H. \tag{10}$$

Here, Ψ_A is obtained by directional averaging of the one-dimensional strain energy $\overset{d}{\Psi}_A$ from Eq. (4) in to three-dimensions.[11] Such directional averaging schemes are now becoming common for modelling open-porous cellular materials.[16,24] In our previous model, the network decomposition was defined as a function of the pore-sizes. There, the smaller pores formed a hydrogel-like network, and with increased hydration, more smaller pores transformed into a hydrogel-like state. Now, Eq. 10 and the presented model show that such dependency of the network decomposition model no longer exits. This is in good agreement with the experimental observations. The focal points can be arbitrarily located through the network. It must also be noted that hydration influences the fibril characteristics in the dry aerogel network. There, the fibrils swell and become thicker, while the Young's modulus of teh fibril becomes softer.

The model comprises of seven material parameters, those that are listed in Table 1. In the following, we first analyse the sensitivity of changes to these parameters towards the macroscopic constitutive behaviour. These are illustrated in Fig. 3. l_{max} has a substantial influence on the macroscopic stiffness of the material. This is due to the fact that higher l_{max} results in the higher $\bar{r}$, which induces the rapid formation of the hydrogel-like network having stiffer characteristics in the hydrated aerogel net-

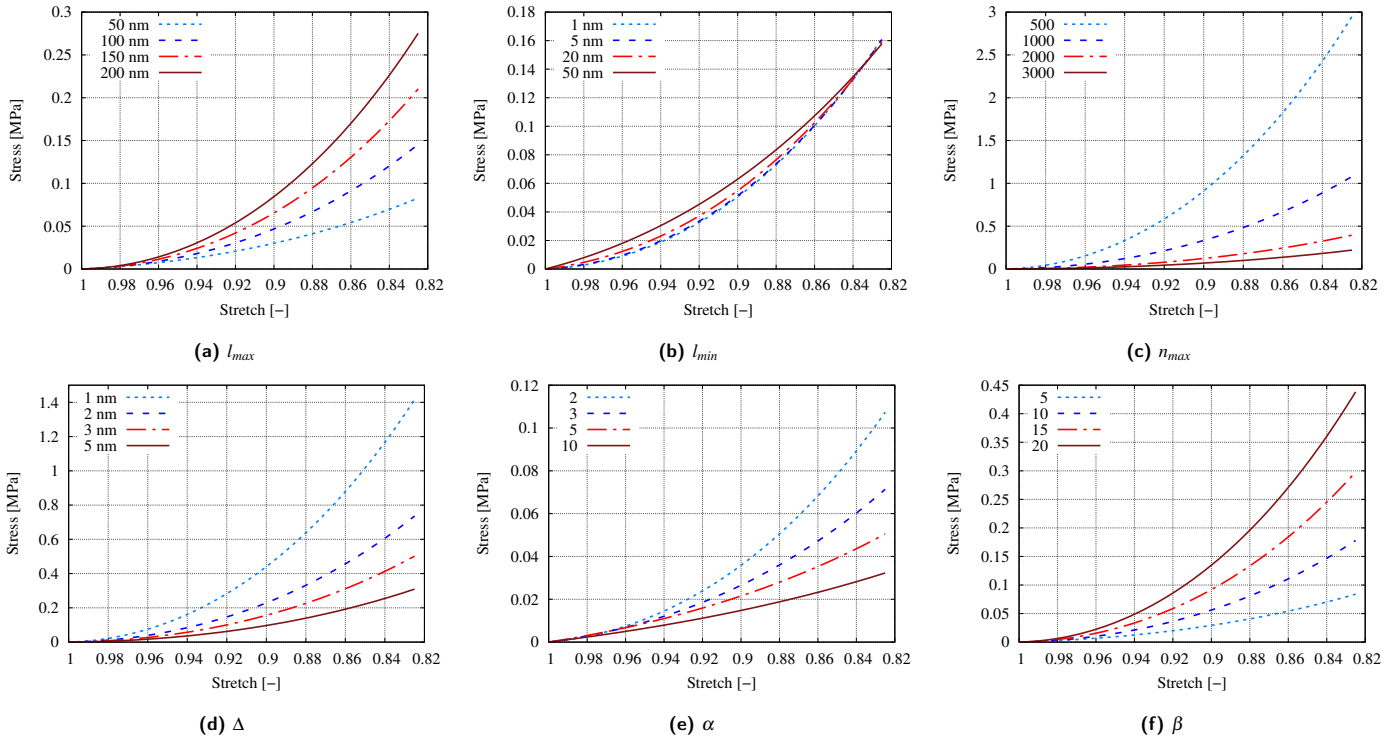

(a) l_{max} **(b)** l_{min} **(c)** n_{max}

(d) Δ **(e)** α **(f)** β

Fig. 3 Sensitivity analysis of the model parameters on the macroscopic constitutive behaviour.

Table 1 The list of material parameters

Material parameter	Description
l_{min}, l_{max}	minimum and maximum fibril lengths
E	Young's modulus
d_F	diameter of fibrils
N_0	initial number of cells
n_{max}	maximum number of segments in a chain of the hydrogel-like network
ν	sliding ratio of the hydrogel-like network chain

work. Changes to l_{min} do not significantly influence the macroscopic behaviour, although, upon close observation, a trend similar to l_{max} can be observed. Δ is inversely proportional to $\bar{r}$, and smaller Δ generates stiffer material. Shorter chains culminate in the higher stress response, which is reciprocally correlated with the n_{max}. The probability density function of the pore-sizes has a significant impact on the stiffness of the material. The behaviour of the shape parameters α and β show an opposite nature upon increment. This shows that, with a higher density of smaller pores in the original network, the higher the probability of obtaining a stiffer mechanical response. Thus, the effect of different parameters can be understood by analysing the plots in Fig. 3.

Of special importance is to evaluate the macroscopic mechanical behaviour under different degrees of wetting. Fig. 4 shows the macroscopic compressive behaviour of the aerogel subject to different degrees of hydration. The pronounced stiffening is effectively captured by the model. As the hydration is increased, the model captured the typical J-shaped nature observed in pure hydrogels. It must be noted, that while calculating the impact of wetting, ξ is also varied along with $\mathscr{H}$. This is because the two parameters are correlated as shown earlier[9] (see Fig. 2).

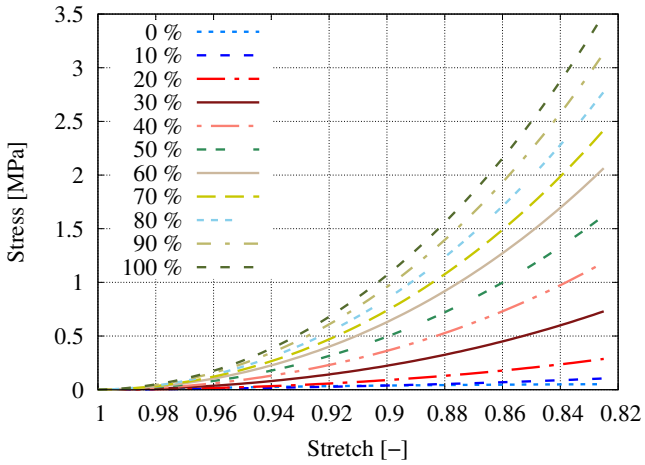

Fig. 4 The effect of hydration in the model. Here, only the parameters $\mathscr{H}$ and correspondingly ξ are changed to account for different degrees of wetting.

Finally, comparison of the model with experimental data of dry, 20% hydrated and 50% hydrated aerogel networks is shown in Fig. 5. By varying only $\mathscr{H}$ and ξ with respect to experimental data while keeping material parameters shown in Table 1 constant, good agreement between the model and experimental data is achieved. This demonstrates the micromechanical nature of the model, which then requires no parameter fitting. These results

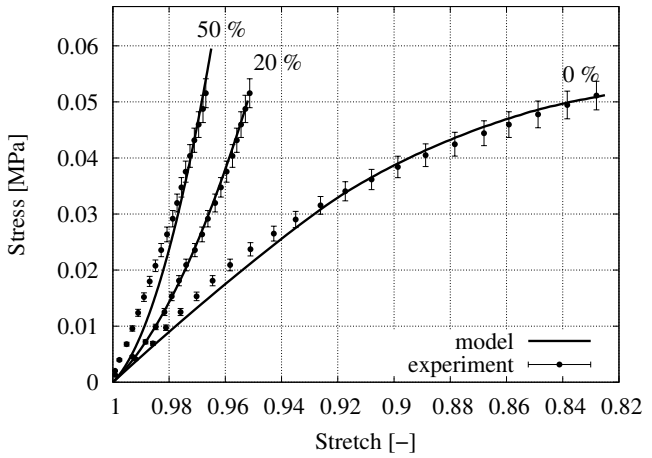

Fig. 5 Comparison of the model predictions with available experimental data.

are very promising in the development of models for describing the hydration effects in nanoporous networks. Further mechanical tests characterising the cyclic behaviour under compression are necessary to investigate the inelastic effects.

Conflicts of interest

There are no conflicts to declare.

Acknowledgements

The authors acknowledge the COST Action CA18125 "Advanced Engineering and Research of aeroGels for Environment and Life Sciences (AERoGELS) for the Short Term Scientific Mission (STSM) program awarded to İ. D. K. The authors also thank Pavel Gurikov from Hamburg University of Technology, Germany and József Kalmár from the University of Debrecen, Hungary for the fruitful discussions.

References

1 S. Zhao, W. J. Malfait, N. Guerrero-Alburquerque, M. M. Koebel and G. Nyström, *Angewandte Chemie International Edition*, 2018, **57**, 7850–7608.

2 C. A. Garcia-Gonzalez, T. Budtova, L. Duraes, C. Erkey, P. Del Gaudio, P. Gurikov, M. Koebel, F. Liebner, M. Neagu and I. Smirnova, *Molecules*, 2019, **24**, year.

3 M. Martins, A. A. Barros, S. Quraishi, P. Gurikov, S. Raman, I. Smirnova, A. R. C. Duarte and R. L. Reis, *The Journal of Supercritical Fluids*, 2015, **106**, 152–159.

4 S. Zhao, W. J. Malfait, A. Demilecamps, Y. Zhang, S. Brunner, L. Huber, P. Tingaut, A. Rigacci, T. Budtova and M. M. Koebel, *Angewandte Chemie*, 2015, **127**, 14490–14494.

5 P. Paraskevopoulou, P. Gurikov, G. Raptopoulos, D. Chriti, M. Papastergiou, Z. Kypritidou, V. Skounakis and A. Argyraki, *Polyhedron*, 2018, **154**, 209–216.

6 V. Santos-Rosales, G. Alvarez-Rivera, M. Hillgärtner, A. Cifuentes, M. Itskov, C. A. García-González and A. Rege, *Biomacromolecules*, 2020, **21**, 5336–5344.

7 S. Antonyuk, S. Heinrich, P. Gurikov, S. Raman and I. Smirnova, *Powder technology*, 2015, **285**, 34–43.

8 A. Rege, L. Ratke, İ. D. Külcü and P. Gurikov, *Journal of Non-Crystalline Solids*, 2020, **531**, 119859.

9 A. Forgács, V. Papp, G. Paul, L. Marchese, A. Len, Z. Dudás, I. Fábián, P. Gurikov and J. Kalmár, *ACS applied materials & interfaces*, 2021, **13**, 2997–3010.

10 H. Schott, *Journal of Macromolecular Science, Part B*, 1992, **31**, 1–9.

11 A. Rege, M. Schestakow, I. Karadagli, L. Ratke and M. Itskov, *Soft Matter*, 2016, **12**, 7079–7088.

12 A. N. Gent, *Rubber chemistry and technology*, 1996, **69**, 59–61.

13 A. Rege, I. Preibisch, M. Schestakow, K. Ganesan, P. Gurikov, B. Milow, I. Smirnova and M. Itskov, *Materials*, 2018, **11**, 1670.

14 K. Bisshopp and D. Drucker, *Quarterly of Applied Mathematics*, 1945, **3**, 272–275.

15 E. P. Barrett, L. G. Joyner and P. P. Halenda, *Journal of the American Chemical society*, 1951, **73**, 373–380.

16 A. Rege, S. Aney and B. Milow, *revised version under review at Phys. Rev. E*.

17 J.-Y. Sun, X. Zhao, W. R. Illeperuma, O. Chaudhuri, K. H. Oh, D. J. Mooney, J. J. Vlassak and Z. Suo, *Nature*, 2012, **489**, 133–136.

18 İ. D. Külcü, *Results in Physics*, 2019, **12**, 1826–1833.

19 E. M. Arruda and M. C. Boyce, *Journal of the Mechanics and Physics of Solids*, 1993, **41**, 389–412.

20 İ. D. Külcü, *Gels*, 2021, **7**, 3.

21 M. Puso, *PhD thesis*, University of California, Davis, 2003.

22 R. Dargazany and M. Itskov, *International Journal of Solids and Structures*, 2009, **46**, 2967–2977.

23 G. Marckmann, E. Verron, L. Gornet, G. Chagnon, P. Charrier and P. Fort, *Journal of the Mechanics and Physics of Solids*, 2002, **50**, 2011–2028.

24 T. Bleistein, A. Jung and S. Diebels, *Continuum Mechanics and Thermodynamics*, 2019.